MATRIX ASSISTED LASER DESORPTION IONIZATION IMAGING MASS SPECTROMETRY: A NEW METHODOLOGY TO STUDY HUMAN OSTEOARTHRITIC CARTILAGE

Berta Cillero Pastor PhD[1], Gert Eijkel[1], Andras Kiss[1], Francisco J. Blanco MD[2], Ron M.A. Heeren PhD[1].

1- Biomolecular Imaging Mass Spectrometry (BIMS) Molecular Nanophotonics Department FOM Institute AMOLF. Amsterdam. The Netherlands.
2- Rheumatology Division. Proteomic Group. Proteo-Red-ISCIII. INIBIC-Hospital Universitario A Coruña, A Coruña, Spain.

This work is part of the research program of the Stichting voor Fundamenteel Onderzoek der Materie (FOM), which is financially supported by the Nederlandse organisatie voor Wetenschappelijk Onderzoek (NWO).
B Cillero-Pastor is the recipient of an Angeles Alvariño grant from Xunta de Galicia.

Correspondence to:
Ron M.A. Heeren, Ph.D.
FOM-Institute AMOLF. Science Park 104. 1098 XG Amsterdam. The Netherlands.
Tel: +31-20-7547100
Fax: +31-20-7547290
Email: heeren@amolf.nl

Running title: Matrix assisted laser desorption ionization imaging mass spectrometry reveals the protein distribution of human osteoarthritic cartilage.

Key words: Fibronectin, Cartilage oligomeric matrix protein, Matrix assisted laser desorption ionization imaging mass spectrometry, Osteoarthritis.

Competing interests: The authors declare that they have no competing interests

Abstract

Objective: The distribution of proteins and the modulation that they undergo in the different phases of rheumatic pathologies is essential to understand the development of these diseases. In this article we demonstrate the utility of MS based molecular imaging to study the spatial distribution of different components in human articular cartilage sections. **Methods**: We have compared the distribution of peptides and proteins in human control and osteoarthritic (OA) cartilage. Human control and OA cartilage slices were cut and deposited on conductivity slides. After tryptic digestion, MALDI-IMS experiments were performed in a MALDI-Q-TOF mass spectrometer. Protein identification was undertaken with a combination of multivariate statistical methods and Mascot protein database queries. Hematoxylin-eosin staining and immunohistochemistry were performed to validate the results. **Results:** We have created maps of peptide distributions at 150 μm pixel size from control and OA human cartilage. Proteins such as biglycan (PGS1), prolargin (PRELP), decorin (PGS2) and aggrecan core protein (PGCA) are identified and localized. Specific protein markers for cartilage oligomeric matrix protein (COMP) and fibronectin (FINC) were exclusively found in the OA samples. Their distribution displayed a stronger intensity in the deep compared to the superficial area. New tentative OA markers were found in the deep area of the OA cartilage. **Conclusions:** MALDI-IMS identifies and localizes disease specific peptides and proteins in cartilage. All the OA related peptides and proteins detected display a stronger intensity in the deep cartilage. Mass spectrometry based molecular imaging is demonstrated to be an innovative method to study OA pathology.

Introduction

Osteoarthritis (OA) is the world most common age related joint disease and is characterized by the degeneration of the cartilage [1, 2]. In addition, degradation processes that structurally change the joint are involved in OA, including synovial inflammation, osteophyte formation, and remodeling of subchondral bone [3]. This pathology affects up to 70% of the population above 65 years of age. Cartilage degradation represents a key process during OA pathogenesis. In addition, treatments to manage OA are limited to control pain and improve function. Therapies to reduce the cartilage degradation and joint destruction are a new challenge in OA treatment. Based in all these comments, methodologies that help us to study in detail the structure of cartilage, could improve the knowledge of OA.

Mass spectrometry (MS) facilitates the molecular identification of lipids, peptides and proteins through the determination of their molecular weight and their fragmentation behavior [4]. Proteins from the cartilage and chondrocytes like prolargin (PRELP), fibromodulin (FMOD), aggrecan core protein (PGCA), decorin (PGS2) or biglycan (PGS1) have been previously identified [5, 6]. All of them interact with glycosaminoglycans and build the extracellular matrix (ECM) in which the chondrocytes are embedded [6]. OA related proteins like COMP and fibronectin (FINC) have been detected by MS and are considered as markers of inflammation and tissue remodeling [7]. None of these proteins have been previously detected and localized in parallel in the same sample, with high spatial resolution and without any type of labeling.

Matrix assisted laser desorption ionization imaging mass spectrometry (MALDI-IMS) can determine the distribution of hundreds of unknown compounds in a single molecular imaging measurement. MALDI-IMS has been used in the last years to look for peptides, proteins and lipids in specific areas of a tissue section with a spatial resolution below 50 μm [4, 8, 9]. After careful preparation the tissue section is introduced in the mass spectrometer and then, the proteins, peptides and lipids are desorbed from discrete pixels from the surface and in an

ordered way. Each pixel is linked to the mass spectrum specific from that region. A plot of the intensity of a signal produces a map of the relative abundance of that compound over the imaged tissue [10]. This technology provides a powerful tool for the investigation of biological processes as it is not known in advance which segment of the molecular complexity will be revealed. IMS is not necessarily a targeted analytical method and technology has been applied to a variety of pathologies such as neurodegenerative disorders and many cancer types [11, 12]. In addition, specific protein patterns revealed by IMS have been shown to be predictive of diagnosis and prognosis [13-15]. MALDI-IMS has been also employed to detect and map pharmaceutical compounds in sections from dosed tissues [14, 15]. Although this is a promising method, there are no previous studies that describe and compare the peptide distribution in human control and OA cartilage. Imaging mass spectrometry is a new technology that can help us localize and identify the key molecules in the OA pathology.

Methods

Materials

α-Cyano-4-hydroxycinnamic acid (HCCA), trifluoroacetic acid (TFA), trypsin and chloroform were obtained from Sigma-Aldrich (Zwijndrecht, The Netherlands). Acetonitrile (ACN) and ethanol were purchased from Biosolve (Westford, MA, USA) and octyl glucoside from Sigma-Aldrich.

Cartilage procurement and processing

Control human knee cartilage from adult donors with no history of joint disease was provided by the Tissue Bank and the Autopsy Service at CHU de La Coruña, Spain. The cartilage was macroscopically and histologically normal. Osteoarthritic (OA) cartilage was obtained from consenting donors who were undergoing joint replacement. Cartilage slices were removed from the condyles and frozen in liquid N_2. 10 µm thick slices were cut in a cryostate and deposited

on indium tin oxide (ITO) high conductivity slides (Delta Technologies, CO, USA) and then frozen at -20ºC. This study was approved by the local ethics committee in Galicia, Spain.

Tissue digestion and matrix deposition for MALDI-IMS

Cartilage samples of ten OA (51-84 years-old) and ten control human donors (51-91 years-old) were studied in duplicate. **Supplementary figure 1** shows the workflow followed. The sections were washed 30 sec. in EtOH 100%, 2 min in EtOH 70% and 30 sec in chloroform. A cocktail of trypsin 50 ng/μL and octyl glucoside 0.01% was applied in an automated fashion (CHIP-1000; Shimadzu Biotech, Kyoto, Japan) [8, 16]. The whole tissue section was microspotted with the enzyme in a 150 μm spacing raster scheme. 20 nL of trypsin per position were deposited in cycles of 250 pL per droplet to cover the entire tissue surface. The samples were incubated overnight at 37ºC. Subsequently, the matrix solution, HCCA (10 mg/mL) in 50% AcN, 50% TFA 0.1% (1:1 vol./vol.), was sprayed on top of the tissue section by a vibrational sprayer (ImagePrep; Bruker Daltonik GmbH, Bremen, Germany).

MALDI–IMS

Digital optical scans of all tissue sections were obtained prior to MALDI–IMS experiments using a 2400 dpi desktop scanner. The resulting digital images were imported into the MALDI Imaging Pattern Creator software (Waters Corporation, Manchester, UK). Instrument calibration was performed using a standard calibration mixture of polyethylene glycol with a M_w of 100-3000 (Sigma-Aldrich). A MALDI SYNAPT™HDMS system (Waters Corporation) operating with a 200 Hz Nd:YAG laser was configured to acquire data in the positive V-reflectron mode. Data were acquired using a laser beam diameter of 150 μm and at a raster size of 150 μm. Ion images were generated with the Biomap 3.7.5.5 software (Novartis Pharma AG, Basel, Sweden).

Tissue digestion and matrix deposition for profiling experiments

Profiling experiments for protein identification were performed on each donor tissue, applying 20 µL of trypsin 0.05 µg/µL and Octyl glucoside 0.01% in water. After drying, 20 µL of matrix was spotted on the digested position. Data dependent analysis (DDA) of tryptic peptides was performed in a MALDI-Q-TOF instrument (Synapt, Waters, UK). Every MS survey scan was followed by collisional fragmentation of the most intense ions and collection of MS/MS spectra. Direct MS/MS fragmentations were performed in those masses directly from the tissue on the peptides that differentiate the OA tissue from the control tissue. These target peptides were found after Discriminant Analysis (DA) of the entire dataset. The obtained spectra were processed in MassLynx™ (Waters Corporation). The resulting data files were submitted to a Mascot (Matrix Science, Boston, MA, USA) search using the Swissprot database.

Multivariate analysis and data interpretation

The intensity of all m/z channels was normalized to the intensity of the m/z 190 matrix peak using Biomap. Peak average intensities were calculated for each mass of interest. Principal Component Analysis (PCA) was used to investigate spectral similarities and differences between all samples studied. The PCA extracted linear combinations of variables, each of which is associated with the largest possible variance after removing the variance of prior principal components in an iterative fashion. The final data analysis was performed with the principal components that explained the highest variance in the data set (80%). Discriminant analysis was performed to look for the peaks with the highest differences between control and diseased groups. P values for statistical differences found in MALDI-IMS and immunohistochemistry experiments were calculated with the Mann-Whitney U test using GraphPad Prism version 5.00 for Macintosh (GraphPad Software, San Diego California USA). Differences were

considered to be statistically significant at P≤0.05. The data were expressed as mean intensity±standard error mean (SEM). String software 9.0 (http://string-db.org/) was used to create hypothetical maps of interactions among different proteins according to PubMed literature.

Immunohistochemistry and morphological studies

Four micrometer thick tissue sections were fixed in acetone (4°C) for 10 min and washed twice in 10 mM phosphate buffered saline, Tween 20 (0.1%) (Sigma-Aldrich). The slides were incubated in a peroxidase blocking solution for 10 min (Dako, Heverlee, Belgium) prior to fibronectin (FINC) immunohistochemistry studies. After rinsing, 100 µl of 1:100 diluted FINC-HRP (IST-9, sc-59826) (Santa Cruz Biotechnology, Heidelberg, Germany) was applied and incubated in a humidified chamber for 1 h at room temperature. The slides were washed in water and 100 µl of a DAB substrate (Dako) was applied for 10 min. The slides were rinsed with water, dehydrated and mounted. Digital images were generated with a BX61 Olympus connected to a DP71 Olympus camera (Olympus Biosystems, Hamburg, Germany). The quantitation was performed with AnalySIS 5.0 software (Olympus Biosystems, Hamburg, Germany). For nuclei and cytoplasm staining, the slides were immersed in Harris hematoxylin solution (Sigma-Aldrich) for 8 minutes. After washing with water, they were rinsed in EtOH 95% and counterstained in an eosin solution for 30 seconds. Digital images were acquired with the Mirax system (Carl Zeiss, Siledrecht, The Netherlands) after dehydrating steps.

Results

MALDI-IMS of control and OA human cartilage samples

MALDI-IMS was used for the study of peptide distributions in control and OA cartilages. A combined spectrum of a representative digested human control

sample is shown in the **supplementary figure 2A**. We detected peaks between 100 and 3000 Da including very abundant peptides, identified by MS/MS in the profiling experiments, such as m/z 1590.90 (PRELP), m/z 2270.20 (PGCA), m/z 2763.30 (PGS2), m/z 2846.30, m/z 3081.60 (PGS1) (**table 1**).

The spectra of a human OA cartilage exhibited a different profile (**supplementary figure 2B**). Several peaks were common to both sample types, such as tryptic peptides of PGS1 and PGCA. Peptides such as FINC (m/z 1349.72, m/z 1593.87), COMP (m/z 2256.15), FMOD (m/z 1955.07), collagen alpha 1 (II) chain (m/z 2023.94) and protein ELYS (m/z 1025.65) were identified by MS/MS directly from the tissue surface (**table 1**) and found to be distinctive for OA.

The images of the peaks were used to investigate the protein distribution differences in OA and control samples through the examination of the tryptic peptide intensities. **Figure 1A** shows a hematoxylin-eosin staining of a control cartilage showing the superficial and the deep area. **Figure 1B** shows the representation of two homogeneously distributed peaks on a control tissue section, one of them corresponding to the protein PRELP (m/z 1590.9). Studying the intensities of some OA specific peptides with the Biomap software, we observed a striking difference in the peak intensity distribution. Four peptides from FINC were imaged in OA and control samples (**Figure 2**). We observed a difference in the normalized intensity of these peaks, using the same scale bar for all figures. First of all, we observed higher intensities of the FINC related peaks in the OA samples. In addition, all of them were predominantly observed in the deep area of the OA cartilage. The tryptic peptides from COMP m/z 2256.1, and m/z 1613.8, exhibited the same pattern differences when control and OA samples were compared (**Figure 3**).

PCA-DA and potential OA markers

DA was employed to generate a target list for tandem mass spectrometry analysis. All the spectra generated in the IMS experiments from control and OA

donors were combined and peak picked prior to PCA. Peak picking was required to reduce the dataset to a size that enables the computational methods needed. DA was performed on the PCs that described 80% of the total variance in the dataset. The remaining variance was discarded as noise. The resulting discriminant functions (DFs) classified the data in two groups: control and OA (**figure 4A**). **Figure 4B** displays the factor spectra and reveals that the peaks of the positive part of the DF1 were specific from OA samples whereas the peaks of negative part were more abundant in control samples. After this analysis, the peaks with the highest absolute loadings, were selected to create a list of OA specific peptides (**supplementary table 1**). These peaks constituted prime candidates for identification through tandem MS analysis. In several cases the signal intensity was not sufficient to perform tandem MS analysis. Interestingly, the table shows that the first four identified masses correspond to tryptic peptides of FINC and their isotopes. We also identified the peak at m/z 1954.0 as a unique peptide from cartilage intermediate layer protein 1 (CILP1). We subsequently examined the distribution of two of these OA specific peaks (m/z 2574.4 and m/z 2376.3) in an OA sample using the Biomap software. This analysis confirmed their predominant localization in the deep area (**supplementary figure 3A**). Using our in-house developed ChemomeTricks software, we plotted all these OA-peak scores to study their localization. The reconstruction of the image showed that the intensities were higher in the deep area of the cartilage rather than in the superficial (**supplementary figure 3B**). In the scale bar the red color represents the highest signal. The figure shows how the abundance progressively changes from the deep to the superficial area in the OA sample. The presence of those peptides in the control sample exhibited a pronounced decrease in comparison to OA. In **supplementary figure 4** the intensity histograms of OA related peaks m/z 1349.7 (**A**) and m/z 2373.7 (**B**) were plotted. The maximum intensity observed in the control samples is much lower than in the OA samples. Moreover in the OA samples we can distinguish two different distributions: the first one with a lower intensity (but higher than the intensities of

the control distribution) and the second one with a higher intensity, showing heterogeneity of peptide distribution that we find in OA samples.

We quantified the differences found in the distribution of two FINC peptides with the Biomap software. The highest intensity differences in the FINC peptide at m/z 1401.7 between control and OA samples were found between the deep areas. In the deep area of the control samples a m/z 1401.7 mean intensity of 0.16±0.02 (SEM) was found versus a mean intensity of 0.47±0.08 in the deep area of the OA tissue (n=10; &*P*<0.01, **figure 5A**). Similar differences in the FINC peptide m/z 1349.7 between control and OA samples were found. The mean intensity of m/z 1349.7 was found to be 0.24±0.05 in the deep area of the control cartilage versus 1.00±0.48 in the deep area of the OA cartilage (n=10; **P*<0.05). In addition to these differences between control and OA samples we observed distinctive intensity differences between the superficial and deep areas in OA samples of the same peaks. We found a mean intensity at m/z 1401.7 of 0.26±0.05 in the superficial area compared to 0.47±0.08 in the deep area (n=10; &*P*<0.01). Similarly, the mean intensity of m/z 1349.7 was 0.62±0.29 in the superficial area versus 1.00±0.48 in the deep area (n=10; **P*<0.05) of the OA tissue (**figure 5B**).

Immunohistochemistry validation of the peptide distribution

The molecular imaging analysis described in the previous sections, revealed a higher intensity of OA related peaks in the deep area of the cartilage. An immunohistochemical staining against FINC was performed to orthogonally validate the results found by IMS. The **figure 5C** shows a immunohistochemistry experiment of FINC, with a hematoxylin counterstain, confiriming an important increase in the deep area of the OA cartilage. The graph of the **figure 5D** represents the average of the FINC positive pixels in the deep area of the OA and control samples, confirming the differences found in the MALDI-IMS approach (mean±SEM 0.2±0.00% control vs. 0.71±0.32% OA; n=3, *P**<0.05).

Discussion

In this study, we have developed a novel protocol to identify and localize peptides/proteins in human control and OA cartilage by MALDI-IMS [17]. MALDI-IMS involves the visualization of the spatial distribution of proteins, peptides or drug compounds within thin slices of samples. It is a promising tool for putative biomarker characterization and drug development. Many authors have already used MALDI-IMS to localize proteins, peptides and lipids in diseased tissues [13, 18]. For instance MALDI-IMS has revealed novel prognostic markers in Barret´s adenocarcinoma, intestinal gastric cancer and it has even used for tumor classification [11, 13, 19-22]. However, nothing has been described until now in relation to rheumatic pathologies.

For the first time we have studied the distribution of peptides in healthy and OA human cartilage by MALDI-IMS. Among the proteins in healthy cartilage, we have identified unique peptides of PGCA (m/z 2271.1, m/z 1315.6, m/z 2270.2), PGS2 (m/z 2763.3), PRELP (m/z 1590.9, m/z 1352.67) or PGS1 (m/z 2027.1, m/z 1312.7, m/z 3081.6, m/z 2846.3). We have shown an example of the homogeneous distribution of the m/z 1590.9 from PRELP and m/z 2278.1 in healthy samples. We have seen a similar distribution of PRELP in OA cartilage (data not shown). All these identified proteins interact with glycosaminoglycans and build the ECM in which the chondrocytes are embedded [23] and modulate collagen fibril formation, especially collagen I, and prevents mineralization of cartilage [24, 25].

In OA samples we have also identified peptides from PGCA (m/z 819.4), PGS1 (m/z 2027.1, m/z 2846.4) and PRELP (m/z 1044.5, m/z 1590.9, m/z 1070.6), collagen alpha 1(II) chain (m/z 2023.9) and ELYS (m/z 1025.6) but also FMOD (m/z 1055.07, m/z 1361.7, m/z 767.4, m/z 978.7). Under pathological conditions, FMOD can activate classical pathways of direct complement binding and plays a role in the inflammation of the joint [26].

Regarding the already known OA related proteins, described in the literature, we have identified different peptides of COMP in OA samples. Our

results indicate a higher presence of the peptides m/z 2256.1 and m/z 1613.8 in OA vs. healthy cartilage. In addition, the distribution in OA cartilage was more abundant in the deep area of the cartilage than in the superficial area [27]. Our findings are consistent with the observation that RA and OA patients that have high levels of COMP in serum, are also positive for bone erosion [28]. Skiöldebrand et al. demonstrated that galloping horses presented a high COMP mRNA expression and protein abundance in the deep areas of osteochondral fragments from the middle carpal joint [29]. By classical proteomics like liquid chromatography (LC), FINC or COMP can be detected in control sample synovial fluid but in a lower concentration than in OA [30, 31]. In our approach we did not perform any protein separation, identifying the proteins directly from the cartilage tissue. COMP is an integral structural component of the cartilage matrix binding to types I, II and IX collagen and I/II procollagen. It has been found in high levels in cartilage, synovial fluid and plasma of OA and RA patients [32]. Only few studies looked for the distribution of COMP in the tissues affected by OA. By microscopy, COMP has been shown to be more present in the inter-cellular matrix than inside the chondrocytes [33, 34] and in rabbits with anterior cruciate ligament transection it stains positively in the area surrounding apoptotic chondrocytes [35]. COMP has been related to endochondral ossification in the developing mouse joint exhibiting a gradient reduction to the superficial zone [36]. The two identified peptides are located in the C-terminal end of COMP which binds collagen I, IX and II, and regulates fibril formation. Mutations in the C-terminal, exerts a dominant-negative effect on both intra- and extracellular processes. This ultimately affects the morphology and proliferation of growth plate chondrocytes, eventually leading to chondrodysplasia and reduced long bone growth. The C-terminal end of COMP is also important because it can directly bind to FINC [37].This interaction pathway is shown in supplementary figure 5 where it can be observed that COMP also binds other proteins associated to OA (FMOD, CILP, MMP3, ITGB6 and ITGB8). Thus, by this technique, the identification of peptides in specific areas of a tissue, can be directly linked to the presence of the protein [8, 38].

We have also identified many peptides from other OA related proteins like FINC. Our results indicate a high presence of the peptides m/z 1401.7, m/z 1593.9, m/z 1431.8 and m/z 1323.7 in OA vs. healthy tissues. On top of that, all these masses were more abundant in the deep area of the OA cartilage than in the superficial area. By means of Biomap software we quantified the intensity of the differences in abundance in healthy and OA samples and in superficial and deep areas. We also performed inmunohistochemistry studies that validated these results. FINC is a glycoprotein present at low levels in the ECM of control cartilage and its increase in OA cartilage, produces a change in chondrocyte phenotype and in the activity of metalloproteases [39]. A positive staining of FINC in the superficial area of OA cartilages has been described. However, the authors pointed out the possibility that the observed FINC stain could be due to the penetration of the protein from the synovial fluid into the cartilage [40]. Our results show high levels in the deep area of OA cartilage and other authors have previously shown results in this direction. FINC synthesis was measured by radioimmunoassays in bovine articular explants as well as in chondrocytes showing high levels in the deep area [41]. Recently, FINC has been found in the deep cartilage of equine cartilage and a clear association between the presence of the protein, caspase-3 and apoptosis of chondrocytes has been shown [42]. It is known that FINC fragments from the synovial fluid but also from the OA cartilage contribute to the tissue remodeling, inflammation and cell death. One hypothesis is that some of the peptides found are related to these FINC fragments. However, the antibody used for the immunohistochemistry studies has affinity for the ED-A heparin binding domain and it’s known to be specific for cytoplasmic FINC and not for FINC fragments.

A high abundance of COMP and FINC proteins in the OA cartilage could be expected. However, we would like to reinforce the idea that this is the first time, to our knowledge, that these proteins have been detected and identified by MALDI-IMS in human cartilage. On top of that, we have observed that all the OA markers detected were increased in the deep area of the OA. These results

confirm that the study of different parts of the cartilage can give us valuable information to understand the biological processes during the OA development.

Performing DA we have shown that we can differentiate the peptide profile of OA and control cartilages. Interestingly, the results that we obtained in a training dataset with three healthy and three OA cartilage samples were confirmed when we increased the number of samples to 10 healthy and 10 OA cartilage donors showing the stability of the technique. Some of the most OA abundant peaks correspond to FINC validating even more the capabilities of the technique. One of the OA peptides classified by DA corresponded to CILP1 (m/z 1954.0) (**supplementary table 1**). Our in house developed software localized this mass in the deep area of the cartilage and with a different intensity in OA vs. healthy tissue. CILP1 has been described as an autoantigen in OA pathology and also to be regulated by growth factors like TGFβ [43, 44]. In addition, CILP1 has been found in higher concentrations in the middle and deep areas of aged compared to young cartilages [45].

We used the peptide cutter tool from the Swissprot database in those peaks that we fragmented but that were not identified by the Mascot algorithm. These peaks matched with FINC (m/z 1355.7 and m/z 1357.7), integrin A5 (m/z 2376.3, m/z 2377.3 and m/z 2378.3) and cartilage intermediate layer protein 2 (CILP2) (m/z 2574.4 and m/z 2575.4). Interestingly different members of the integrin family can bind FINC and COMP proteins demonstrating the close relationship that exist between all these proteins [46, 47]. Lorenzo et al. found that CILP2 (C1 isoform) can be used for differentiation of OA from RA and non diseased [48]. All the known and unknown OA related peaks given by DA, were also localized by our in house developed software in the deep area of the cartilage. Biomap software confirmed this distribution as we showed for the peptides m/z 2574.4 and m/z 2376.3.

Graphical representation of the intensity vs. number of pixels of peptides with high scores in the DF1, revealed that their average intensity was higher in OA than in healthy samples. Two different distributions represented the heterogeneity of OA cartilage. This fact demonstrates the capability of MALDI-

IMS to classify different types of tissues according to 1) the score after DA and 2) the representation of the intensity vs. number of pixels for a specific mass.

Some of the proteins that were identified by MS/MS were subjected to a protein interaction analysis using the String software 9.0. This resulted in a theoretical OA protein interaction map. All of the included members (COMP, FINC, CILP1 and FMOD) are connected to different proteins of the integrin family (ITGB5, ITGB3, ITGB7, ITGA5, ITGA2, ITGA3, ITGB8, ITGB1, ITGA4, ITGA2B) (**supplementary figure 5**). Integrins are proteins that connect the cytoskeleton to the ECM. Cell signaling mediated through integrins regulates several chondrocyte functions including differentiation, matrix remodeling and cell survival [49]. Other authors have shown that during OA abnormal integrin expression alters ECM/cell signaling and modifies chondrocytes synthesis with the subsequent imbalance of destructive cytokines [50]. Future experiments to validate the identity of these OA specific masses could reveal these proteins as prime species for diagnosis and potential drug targets. These results suggest the potential of MALDI-IMS for the localization and identification of known but also unknown proteins in the cartilage.

Conclusion: In this work we have simultaneously localized and identified for the first time peptides from human healthy and OA cartilage by MALDI-IMS. The abundance of all the detected OA peptides was higher in the deep than in the superficial area of the OA cartilage. MALDI-IMS provides a new way to study and image molecules in different areas of the cartilage and to understand molecular signaling pathways and the physiology of the OA cartilage in a fast and sensitive way.

Bibliography

1. Fautrel B and Bourgeois P. [Rheumatic disorders. Overview]. Drugs 2000;59 Spec No 1:1-9.
2. Beaupre GS, Stevens SS and Carter DR. Mechanobiology in the development, maintenance, and degeneration of articular cartilage. J Rehabil Res Dev 2000;37:145-51.

3. Enokida M and Teshima R. [Morphological features of articular cartilage and synovial membrane in osteoarthritis and rheumatoid arthritis]. Clin Calcium 2004;14:45-50.
4. Schwamborn K and Caprioli RM. MALDI imaging mass spectrometry--painting molecular pictures. Mol Oncol 2010;4:529-38.
5. Ruiz-Romero C and Blanco FJ. Proteomics role in the search for improved diagnosis, prognosis and treatment of osteoarthritis. Osteoarthritis Cartilage 2010;18:500-9.
6. Wilson R, Belluoccio D and Bateman JF. Proteomic analysis of cartilage proteins. Methods 2008;45:22-31.
7. Zhen EY, Brittain IJ, Laska DA, Mitchell PG, Sumer EU, Karsdal MA, et al. Characterization of metalloprotease cleavage products of human articular cartilage. Arthritis Rheum 2008;58:2420-31.
8. Stauber J, MacAleese L, Franck J, Claude E, Snel M, Kaletas BK, et al. On-tissue protein identification and imaging by MALDI-ion mobility mass spectrometry. J Am Soc Mass Spectrom 2010;21:338-47.
9. Amstalden van Hove ER, Smith DF and Heeren RM. A concise review of mass spectrometry imaging. J Chromatogr A 2010;1217:3946-54.
10. Walch A, Rauser S, Deininger SO and Hofler H. MALDI imaging mass spectrometry for direct tissue analysis: a new frontier for molecular histology. Histochem Cell Biol 2008;130:421-34.
11. Gustafsson JO, Oehler MK, Ruszkiewicz A, McColl SR and Hoffmann P. MALDI Imaging Mass Spectrometry (MALDI-IMS)-Application of Spatial Proteomics for Ovarian Cancer Classification and Diagnosis. Int J Mol Sci 2011;12:773-94.
12. Stauber J, Lemaire R, Franck J, Bonnel D, Croix D, Day R, et al. MALDI imaging of formalin-fixed paraffin-embedded tissues: application to model animals of Parkinson disease for biomarker hunting. J Proteome Res 2008;7:969-78.
13. Balluff B, Rauser S, Meding S, Elsner M, Schone C, Feuchtinger A, et al. MALDI imaging identifies prognostic seven-protein signature of novel tissue markers in intestinal-type gastric cancer. Am J Pathol 2011;179:2720-9.
14. Bunch J, Clench MR and Richards DS. Determination of pharmaceutical compounds in skin by imaging matrix-assisted laser desorption/ionisation mass spectrometry. Rapid Commun Mass Spectrom 2004;18:3051-60.
15. Hsieh Y, Chen J and Korfmacher WA. Mapping pharmaceuticals in tissues using MALDI imaging mass spectrometry. J Pharmacol Toxicol Methods 2007;55:193-200.
16. Kaletas BK, van der Wiel IM, Stauber J, Guzel C, Kros JM, Luider TM, et al. Sample preparation issues for tissue imaging by imaging MS. Proteomics 2009;9:2622-33.
17. McDonnell LA and Heeren RM. Imaging mass spectrometry. Mass Spectrom Rev 2007;26:606-43.
18. Rauser S, Marquardt C, Balluff B, Deininger SO, Albers C, Belau E, et al. Classification of HER2 receptor status in breast cancer tissues by MALDI imaging mass spectrometry. J Proteome Res 2010;9:1854-63.

19. Elsner M, Rauser S, Maier S, Schone C, Balluff B, Meding S, et al. MALDI imaging mass spectrometry reveals COX7A2, TAGLN2 and S100-A10 as novel prognostic markers in Barrett's adenocarcinoma. J Proteomics 2012.
20. Meding S, Nitsche U, Balluff B, Elsner M, Rauser S, Schone C, et al. Tumor Classification of Six Common Cancer Types Based on Proteomic Profiling by MALDI Imaging. J Proteome Res 2012;11:1996-2003.
21. Hanrieder J, Ljungdahl A, Falth M, Mammo SE, Bergquist J and Andersson M. L-DOPA-induced dyskinesia is associated with regional increase of striatal dynorphin peptides as elucidated by imaging mass spectrometry. Mol Cell Proteomics 2011;10:M111 009308.
22. El Ayed M, Bonnel D, Longuespee R, Castelier C, Franck J, Vergara D, et al. MALDI imaging mass spectrometry in ovarian cancer for tracking, identifying, and validating biomarkers. Med Sci Monit 2010;16:BR233-45.
23. Hyc A, Osiecka-Iwan A, Jozwiak J and Moskalewski S. The morphology and selected biological properties of articular cartilage. Ortop Traumatol Rehabil 2001;3:151-62.
24. Hedlund H, Mengarelli-Widholm S, Heinegard D, Reinholt FP and Svensson O. Fibromodulin distribution and association with collagen. Matrix Biol 1994;14:227-32.
25. Heinegard D and Oldberg A. Structure and biology of cartilage and bone matrix noncollagenous macromolecules. FASEB J 1989;3:2042-51.
26. Sjoberg A, Onnerfjord P, Morgelin M, Heinegard D and Blom AM. The extracellular matrix and inflammation: fibromodulin activates the classical pathway of complement by directly binding C1q. J Biol Chem 2005;280:32301-8.
27. Pearle AD, Warren RF and Rodeo SA. Basic science of articular cartilage and osteoarthritis. Clin Sports Med 2005;24:1-12.
28. Fujikawa K, Kawakami A, Tamai M, Uetani M, Takao S, Arima K, et al. High serum cartilage oligomeric matrix protein determines the subset of patients with early-stage rheumatoid arthritis with high serum C-reactive protein, matrix metalloproteinase-3, and MRI-proven bone erosion. J Rheumatol 2009;36:1126-9.
29. Skioldebrand E, Heinegard D, Eloranta ML, Nilsson G, Dudhia J, Sandgren B, et al. Enhanced concentration of COMP (cartilage oligomeric matrix protein) in osteochondral fractures from racing Thoroughbreds. J Orthop Res 2005;23:156-63.
30. Clutterbuck AL, Smith JR, Allaway D, Harris P, Liddell S and Mobasheri A. High throughput proteomic analysis of the secretome in an explant model of articular cartilage inflammation. J Proteomics 2011;74:704-15.
31. Stevens AL, Wishnok JS, Chai DH, Grodzinsky AJ and Tannenbaum SR. A sodium dodecyl sulfate-polyacrylamide gel electrophoresis-liquid chromatography tandem mass spectrometry analysis of bovine cartilage tissue response to mechanical compression injury and the inflammatory cytokines tumor necrosis factor alpha and interleukin-1beta. Arthritis Rheum 2008;58:489-500.
32. Recklies AD, Baillargeon L and White C. Regulation of cartilage oligomeric matrix protein synthesis in human synovial cells and articular chondrocytes. Arthritis Rheum 1998;41:997-1006.

33. Ekman S, Reinholt FP, Hultenby K and Heinegard D. Ultrastructural immunolocalization of cartilage oligomeric matrix protein (COMP) in porcine growth cartilage. Calcif Tissue Int 1997;60:547-53.
34. Hedbom E, Antonsson P, Hjerpe A, Aeschlimann D, Paulsson M, Rosa-Pimentel E, et al. Cartilage matrix proteins. An acidic oligomeric protein (COMP) detected only in cartilage. J Biol Chem 1992;267:6132-6.
35. Lopez-Franco M, Lopez-Franco O, Murciano-Anton MA, Canamero-Vaquero M, Herrero-Beaumont G, Fernandez-Acenero MJ, et al. An experimental study of COMP (cartilage oligomeric matrix protein) in the rabbit menisci. Arch Orthop Trauma Surg 2011.
36. Murphy JM, Heinegard R, McIntosh A, Sterchi D and Barry FP. Distribution of cartilage molecules in the developing mouse joint. Matrix Biol 1999;18:487-97.
37. Di Cesare PE, Chen FS, Moergelin M, Carlson CS, Leslie MP, Perris R, et al. Matrix-matrix interaction of cartilage oligomeric matrix protein and fibronectin. Matrix Biol 2002;21:461-70.
38. Cole LM, Djidja MC, Bluff J, Claude E, Carolan VA, Paley M, et al. Investigation of protein induction in tumour vascular targeted strategies by MALDI MSI. Methods 2011;54:442-53.
39. Homandberg GA. Potential regulation of cartilage metabolism in osteoarthritis by fibronectin fragments. Front Biosci 1999;4:D713-30.
40. Rees JA, Ali SY and Brown RA. Ultrastructural localisation of fibronectin in human osteoarthritic articular cartilage. Ann Rheum Dis 1987;46:816-22.
41. Hayashi T, Abe E and Jasin HE. Fibronectin synthesis in superficial and deep layers of normal articular cartilage. Arthritis Rheum 1996;39:567-73.
42. Thomas CM, Murray R and Sharif M. Chondrocyte apoptosis determined by caspase-3 expression varies with fibronectin distribution in equine articular cartilage. Int J Rheum Dis 2011;14:290-7.
43. Du H, Masuko-Hongo K, Nakamura H, Xiang Y, Bao CD, Wang XD, et al. The prevalence of autoantibodies against cartilage intermediate layer protein, YKL-39, osteopontin, and cyclic citrullinated peptide in patients with early-stage knee osteoarthritis: evidence of a variety of autoimmune processes. Rheumatol Int 2005;26:35-41.
44. Mori M, Nakajima M, Mikami Y, Seki S, Takigawa M, Kubo T, et al. Transcriptional regulation of the cartilage intermediate layer protein (CILP) gene. Biochem Biophys Res Commun 2006;341:121-7.
45. Lorenzo P, Bayliss MT and Heinegard D. A novel cartilage protein (CILP) present in the mid-zone of human articular cartilage increases with age. J Biol Chem 1998;273:23463-8.
46. Peters JH, Loredo GA and Benton HP. Is osteoarthritis a 'fibronectin-integrin imbalance disorder'? Osteoarthritis Cartilage 2002;10:831-5.
47. Rock MJ, Holden P, Horton WA and Cohn DH. Cartilage oligomeric matrix protein promotes cell attachment via two independent mechanisms involving CD47 and alphaVbeta3 integrin. Mol Cell Biochem 2010;338:215-24.
48. Lorenzo P ST, Heinegard D, Cartilage intermediate layer protein 2 C1 and its use to differentiate osteoarthritis from rheumatoid arthritis and non-disease conditions. 2010: Lund SE.

49. Loeser RF. Integrins and cell signaling in chondrocytes. Biorheology 2002;39:119-24.
50. Iannone F and Lapadula G. The pathophysiology of osteoarthritis. Aging Clin Exp Res 2003;15:364-72.

Acknowledgments

This work is part of the research program of the Stichting voor Fundamenteel Onderzoek der Materie (FOM), which is financially supported by the Nederlandse organisatie voor Wetenschappelijk Onderzoek (NWO). The authors acknowledge partial support for this work by the Netherlands Proteomics Centre and Xunta de Galicia (Program Ángeles Alvariño)

Figure legends

Figure 1: Analyses of peptide distribution and H&E staining. A) Hematoxylin and eosin staining of an OA sample. The deep area (close to the bone) and the superficial area (in contact with the synovial liquid) are clearly differentiated. B) Example of the distribution of the random peptide m/z 2278.1 and the peptide m/z 1590.9 from the protein PRELP in a control sample after MALDI-IMS experiments. Scale bar shows normalized intensities.

Figure 2: Distribution and intensities of four peptides from the FINC protein in control and OA cartilage. The figure represents the different intensities and distributions of FINC peptides in control and OA samples after MALDI-IMS experiments and MSMS profiling identifications. Scale bar shows normalized intensities.

Figure 3: Comparison of the intensity and the distribution of two peptides from COMP in control and OA cartilage. The figure represents the different intensities and distributions of COMP peptides in control and OA samples after MALDI-IMS experiments and MSMS profiling identifications. Scale bar shows normalized intensities.

Figure 4: PCA and DA. A) The spectra of all the control and OA samples after MALDI-IMS experiments were analyzed by PCA and DA to classify peptides specific of each condition. The positive part of the graph corresponds to OA samples and the negative to control samples. B) Loading plot of DF1 representing the peptides specific of the OA condition given by the MALDI-IMS approach.

Figure 5: FINC validation in control and OA cartilage. A) Biomap was used to quantify the differences in the FINC peptide m/z 1401.7 between control and OA cartilages (mean intensity±SEM, n=10; deep N vs. deep OA=&*P*<0.01, sup OA

vs. deep OA=&P<0.01). B) Biomap software was employed to quantify the differences in intensity of the FINC peptide m/z 1349.7 (mean intensity±SEM, n=10; deep N vs. deep OA=*P<0.05, sup OA vs. deep OA=*P<0.05). C) A representative experiment of hematoxylin eosin staining and FINC immunohistochemistry in control and OA samples is shown. D) Quantitation of differences in FINC positivity between deep areas of control and OA cartilages (mean positivity±SEM, n=3; *P<0.05).

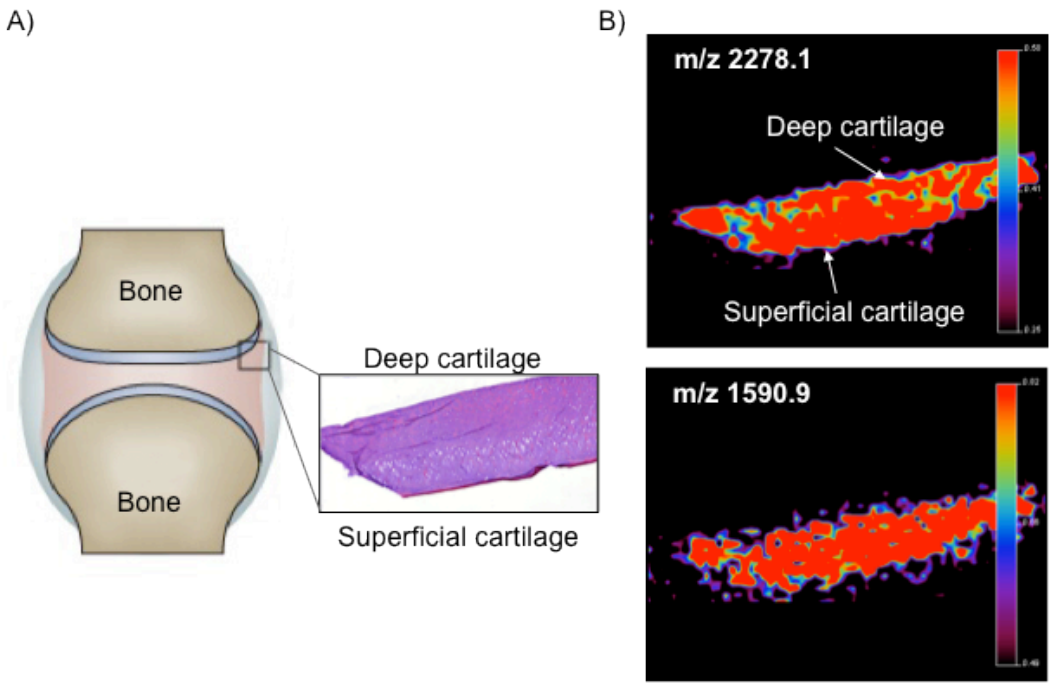

Figure 1: Analyses of peptide distribution and H&E staining. A) Hematoxylin and eosin staining of an OA sample. The deep area (close to the bone) and the superficial area (in contact with the synovial liquid) are clearly differentiated. B) Example of the distribution of the random peptide m/z 2278.1 and the peptide m/z 1590.9 from the protein PRELP in a control sample after MALDI-IMS experiments. Scale bar shows normalized intensities.

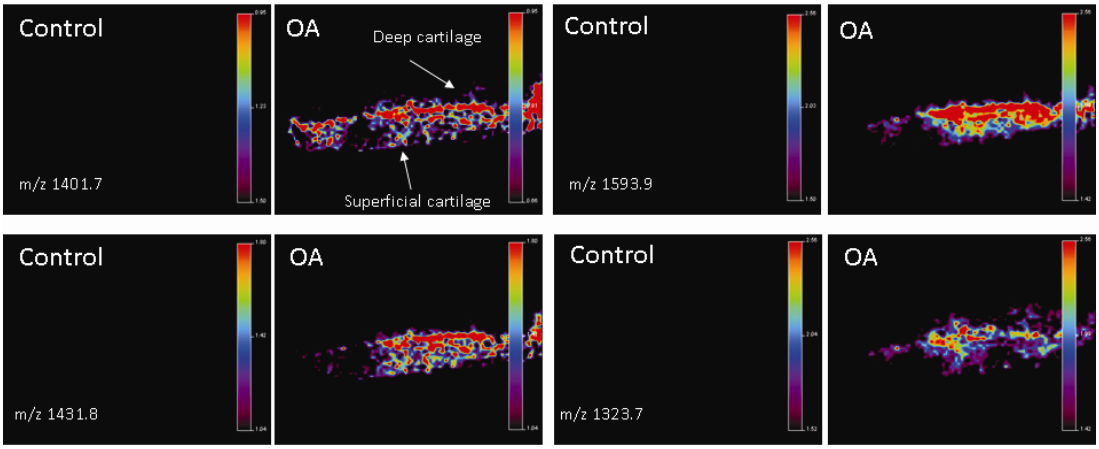

Figure 2: Distribution and intensities of four peptides from the FINC protein in control and OA cartilage. The figure represents the different intensities and distributions of FINC peptides in control and OA samples after MALDI-IMS experiments and MSMS profiling identifications. Scale bar shows normalized intensities.

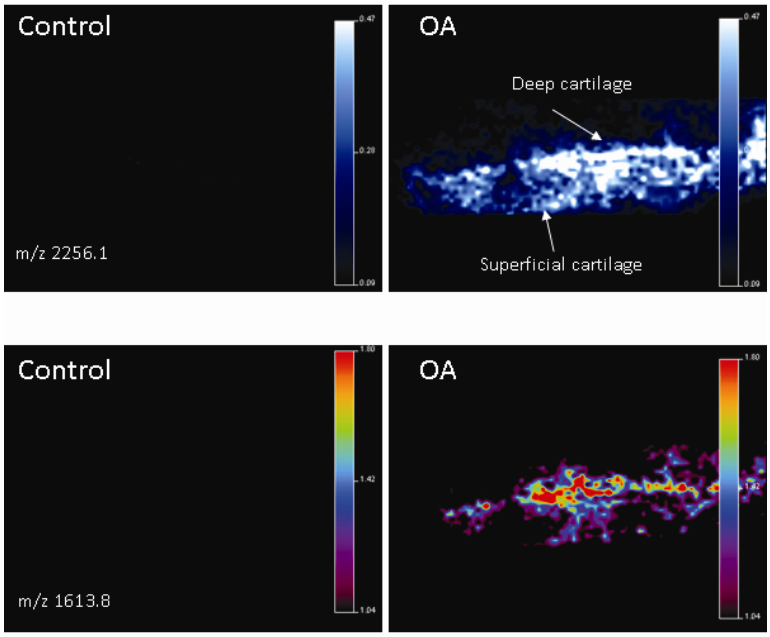

Figure 3: Comparison of the intensity and the distribution of two peptides from COMP in control and OA cartilage. The figure represents the different intensities and distributions of COMP peptides in control and OA samples after MALDI-IMS experiments and MSMS profiling identifications. Scale bar shows normalized intensities.

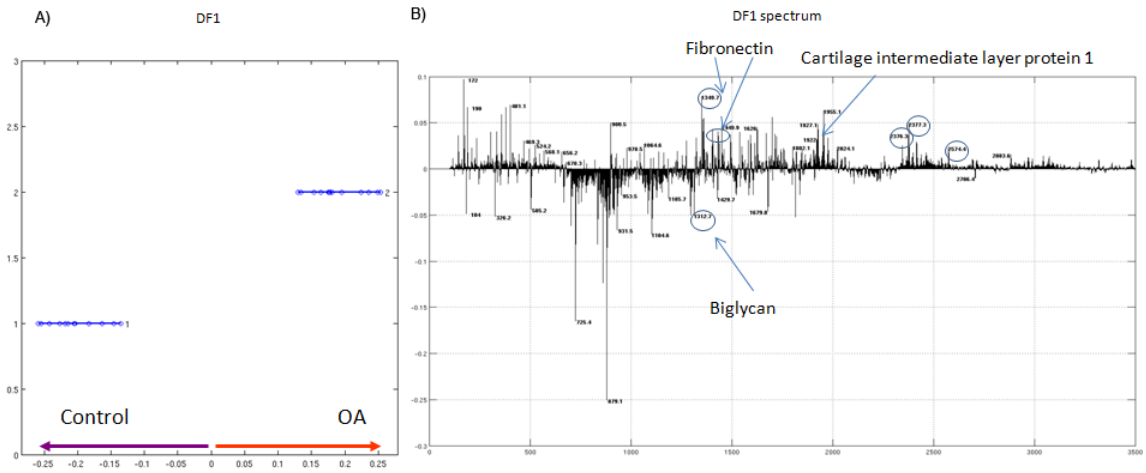

Figure 4: PCA and DA. A) The spectra of all the control and OA samples after MALDI-IMS experiments were analyzed by PCA and DA to classify peptides specific of each condition. The positive part of the graph corresponds to OA samples and the negative to control samples. B) Loading plot of DF1 representing the peptides specific of the OA condition given by the MALDI-IMS approach.

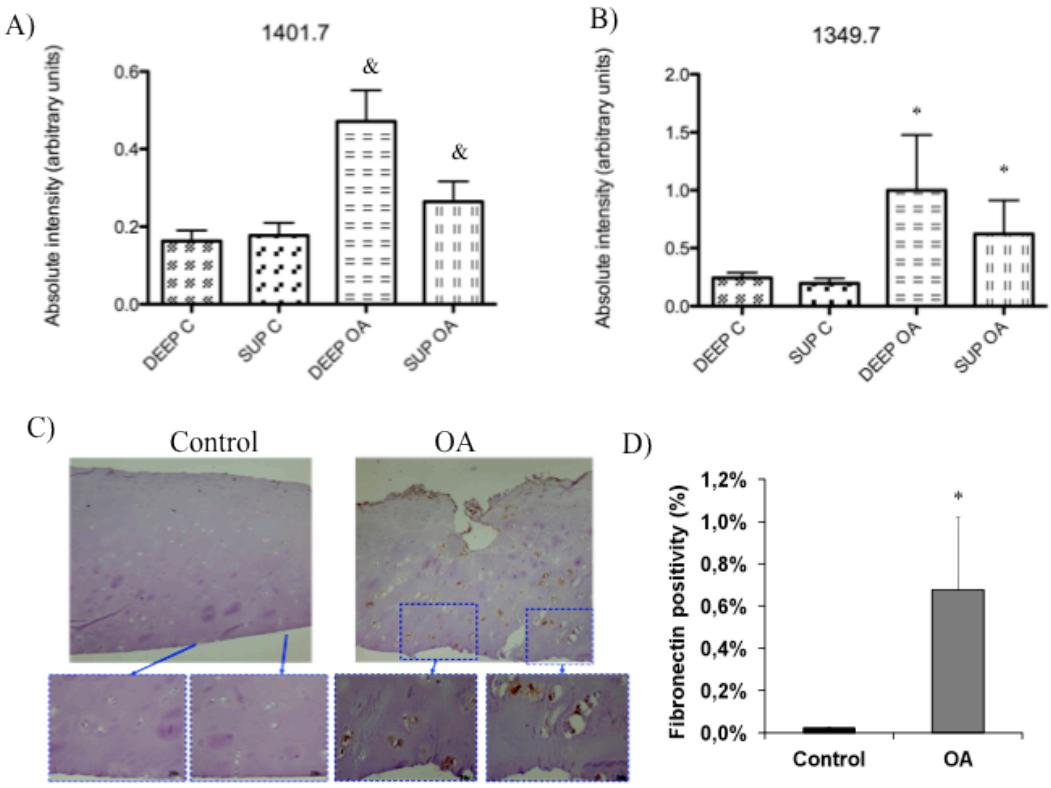

Figure 5: FINC validation in control and OA cartilage. A) Biomap was used to quantify the differences in the FINC peptide m/z 1401.7 between control and OA cartilages (mean intensity±SEM, n=10; deep N vs. deep OA=&*P*<0.01, sup OA vs. deep OA=&P<0.01). B) Biomap software was employed to quantify the differences in intensity of the FINC peptide m/z 1349.7 (mean intensity±SEM, n=10; deep N vs. deep OA=**P*<0.05, sup OA vs. deep OA=*P<0.05). C) A representative experiment of hematoxylin eosin staining and FINC immunohistochemistry in control and OA samples is shown. D) Quantitation of differences in FINC positivity between deep areas of control and OA cartilages (mean positivity±SEM, n=3; **P*<0.05).